

## Polarization rotation of shape resonance in Archimedean spiral slots

Lawrence Dah-Ching Tzuang,<sup>a)</sup> Yu-Wei Jiang, Yi-Han Ye, Yi-Tsung Chang, Yi-Ting Wu, and Si-Chen Lee<sup>b)</sup>

Department of Electrical Engineering, Graduate Institute of Electronics Engineering, National Taiwan University, Taipei 10617, Taiwan

(Received 8 February 2009; accepted 17 February 2009; published online 6 March 2009)

The experimental results of linear polarized light transmitting through an array of Archimedean spiral slots perforated on a thin metal film in the far-infrared region are demonstrated. The wavelength selective transmission spectra are examined, and the polarization selective shape resonance will lead to the polarization rotation. The sign of rotation not only depend on the handedness of the spiral but also related to specific initial polarization position. This phenomenon is different from the conventional optical activity in three-dimensional chiral molecules but rather similar to the polarization selective features in rectangular or elliptical slots. © 2009 American Institute of Physics. [DOI: 10.1063/1.3097023]

Light transmission through a thin metallic film perforated with an array of apertures having reduced symmetry such as elliptical<sup>1</sup> and rectangular<sup>2</sup> shaped holes shows strong polarization effects. As the aperture is sculptured into complex structures such as *c*- or  $\epsilon$ -shape, strong transmission peaks at specific wavelengths larger than the aperture diameter were demonstrated, which is attributed to the localized shape resonance (SR). The individual hole acts as a resonating element, and the array of holes possesses important filtering applications.<sup>3</sup> Therefore, the circular hole can be elongated and wound into planar chiral (a geometrical figure is said to be chiral if its mirror image cannot be brought to coincide with itself) geometries that induce SRs in the transmission spectrum and exhibit strong polarization dependence. The Archimedean spiral is the most typical anisotropic planar chiral geometry and is adopted to measure the polarization dependent transmission in the far-infrared region. The polarization rotation induced by SR is also measured.

The chiral structure can be used to manipulate the polarization state of the incident electromagnetic wave such as circular dichroism and optical activity.<sup>4</sup> Recently, the time reversal debate on planar chiral structure argued that the sense of twist is reversed while looking from the back of the film. This indicates an opposite polarization effect when light propagates backward that lead to an asymmetric propagating effect,<sup>5,6</sup> which is not observed in three-dimensional chiral mediums or in planar chirals with high symmetry such as gammadians.<sup>7-10</sup> However, it is shown in this paper that the polarization rotation induced by SR is a common phenomenon due to its polarization preference and is not completely dependent on the handedness of the spiral. Similar results had been reported by Wickenden *et al.*<sup>11</sup> but they did not go in detail to the mechanism of the rotation, and they studied spiral *wires* in the microwave region, which is fundamentally different from this work. Here, a full picture relating the polarization dependent transmission and rotation for SR will be illustrated.

Figure 1(a) displays the hole array of Archimedean spirals arranged in a square lattice with period  $\Lambda = 21 \mu\text{m}$  per-

forated on 100 nm Ag film evaporated on top of an *n*-type double polished silicon substrate. By using lithography process, the right-handed (RH) [viewing from top of Fig. 1(a) and twisting from the center] spiral slot was patterned with

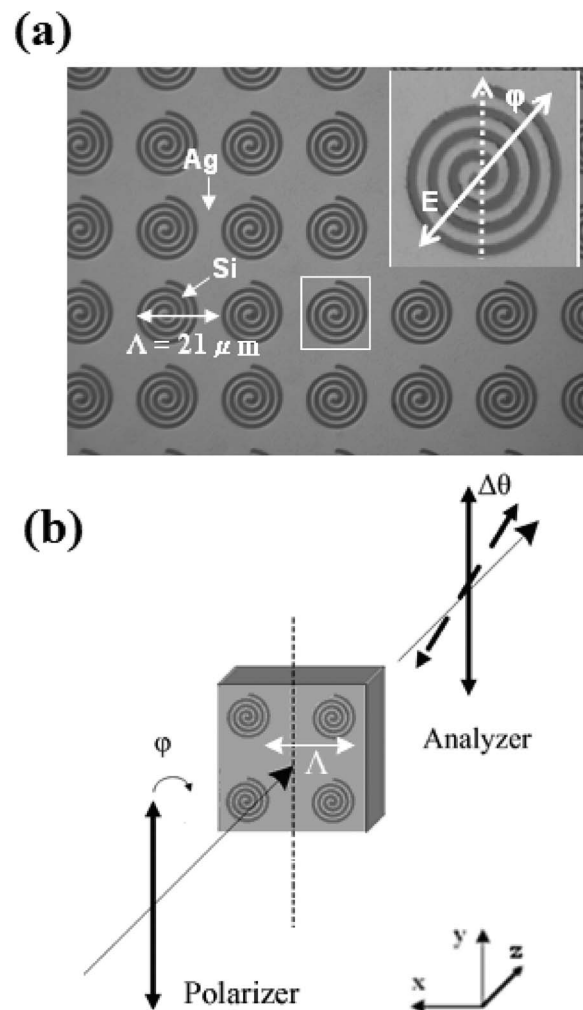


FIG. 1. (a) Top view of an array of spiral slots with 3.5 turn characteristic. The slot and metal widths are all equal to  $1 \mu\text{m}$ . (b) Schematic diagram of the experimental setup.  $\varphi$  denotes the angle of the polarization orientation from *y* axis in *x-y* plane.

<sup>a)</sup>Electronic mail: r95943176@ntu.edu.tw.

<sup>b)</sup>Electronic mail: scllee@cc.ee.ntu.edu.tw.

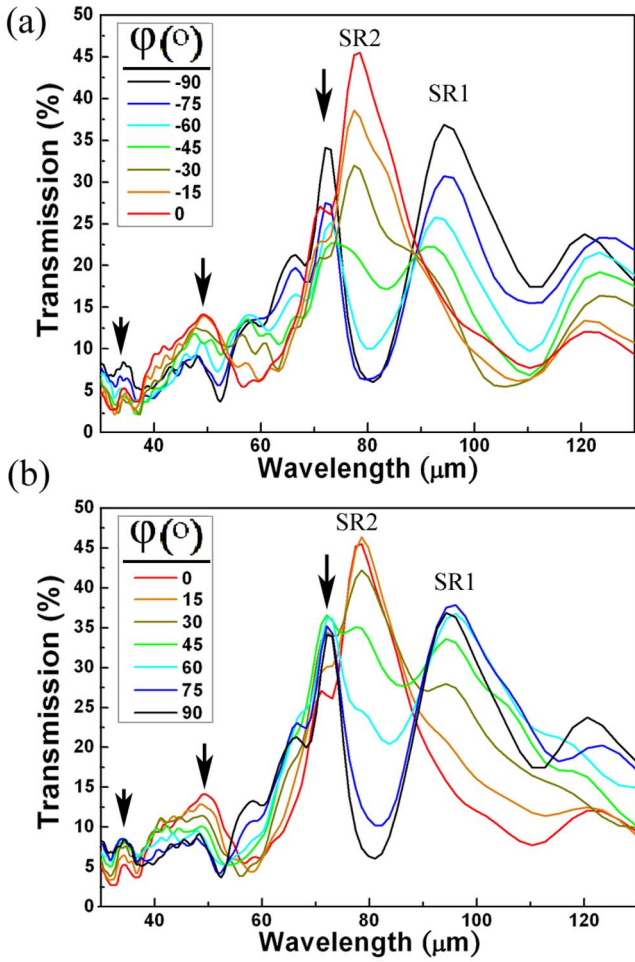


FIG. 2. (Color online) Normal incidence transmission spectra of RH Archimedean spirals arranged in a square lattice with period  $\Lambda=21 \mu\text{m}$  with polarization angle  $\phi$  alternating from (a)  $-90^\circ$  to  $0^\circ$  (polarizer oriented from horizontal to vertical) and from (b)  $0^\circ$  to  $90^\circ$  (polarizer oriented from vertical to horizontal). The vertical arrows denotes the theoretical location of the SPs.

3.5 turn (defined as starting from the inner end of the gap to the outer end) characteristic. The slot and metal width are all  $1 \mu\text{m}$ . The experimental setup is shown in Fig. 1(b), which the sample was placed between a pair of polarizers (polarizer/analyzer) with total sample area of  $5 \times 5 \text{ mm}^2$  and the transmission spectra were measured in a Bruker IFS 66 v/s Fourier-transform infrared spectrometer with a beam size of  $3 \text{ mm}$ . The wavenumber resolution of the measurement is  $8 \text{ cm}^{-1}$ .

The transmission spectra shown in Figs. 2(a) and 2(b) were measured on RH Archimedean spirals arranged in a square lattice with period  $\Lambda=21 \mu\text{m}$  without the analyzer, while rotating polarization azimuth angle  $\phi$  from  $90^\circ$  to  $-90^\circ$  gives different initial polarization states. The vertical arrows denote the theoretical positions of surface plasmon<sup>12</sup> (SP) enhanced transmission. Other peaks are contributed by SRs, among them the two major peaks with the largest transmission are denoted as SR1 and SR2. More evidence on the coexistence of SP and SR from experiments and numerical simulations are verified that the SPs are strongly related to the period of the array, whereas the resonance position of SRs is only dependent on its total slot length and do not alter with oblique incidence of light (not shown). SR1 and SR2 have a maximum transmission at  $\phi \sim 75^\circ$  and  $5^\circ$ , respec-

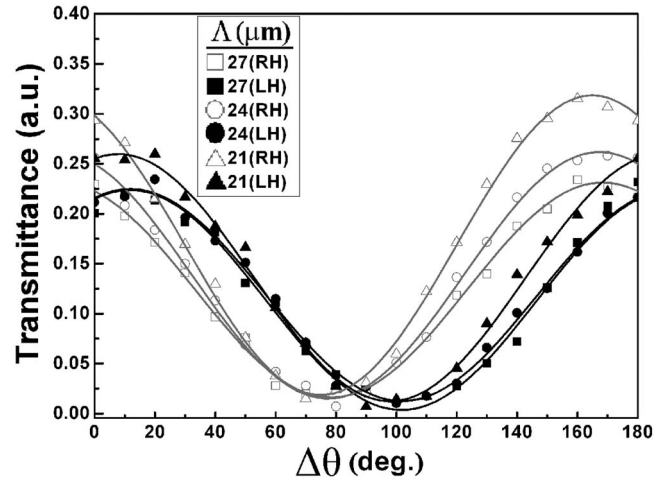


FIG. 3. Measured peak transmittance vs analyzer angle  $\Delta\theta$  for RH and LH with  $\Lambda=27, 24,$  and  $21 \mu\text{m}$  for SR1 at  $\phi=90^\circ$ . The solid curve is the fitting result of Eq. (2) for RH (gray) and LH (black) spirals.

tively. This indicates that an optimized polarization orientation is required to fully excite the corresponding SR mode. This is a unique phenomenon that the polarization dependence is not controlled by the polarization in orthogonal directions but at particular angles that depend on the geometry of the spiral. The pass band at SR1 or SR2 can be switched on or off by alternating the polarization orientation, which provides great potential in polarization controlled filtering application.

Polarization rotation measurements were performed in the presence of an analyzer as illustrated in Fig. 1(b). The intensity of light penetrating through a pair of ideal polarizer with  $\Delta\theta$  between their axes will follow Malus's law,<sup>4</sup>

$$I(\Delta\theta) = I(0)\cos^2 \Delta\theta, \tag{1}$$

where  $I(0)$  is the incident light intensity corresponding to  $\Delta\theta=0$ . By recording the transmission maxima of each spectrum while rotating the analyzer of  $\Delta\theta$  from  $0^\circ$  to  $180^\circ$  in the  $x$ - $y$  plane at  $10^\circ$  increment, the data can be fitted by a modified form of Eq. (1),

$$T = \beta + \gamma \cos^2 \left[ \left( \frac{\Delta\theta - \delta_0}{180^\circ} \right) \pi \right], \tag{2}$$

where  $T$  is the intensity of light transmission,  $\beta$  and  $\gamma$  are fitting parameters, and  $\delta_0$  corresponds to the rotation angle of polarization azimuth for the transmitted light. The magnitude of ellipticity  $|\eta|$  is estimated by calculating the arctangent of the ratio between transmission minimum and maximum that do not point out the handedness ( $\pm$ ) of the elliptical polarization. The calibration on silicon substrate exhibits near null result of  $\delta_0=0.3^\circ$  and  $|\eta|=1.2^\circ$ .

Following the same procedure, Fig. 3 shows the measured peak transmittance for SR1 at  $94 \mu\text{m}$  with initial polarization state at  $\phi=90^\circ$  as a function of  $\Delta\theta$ . Left-handed (LH) spirals are measured with a horizontally flip of the original RH sample in Fig. 1(b). Note that the perceived handedness alters from RH to LH spirals when light impinges from the back, which is independent on the position of the silicon substrate. The results on RH and LH spirals were separated by colors of gray and black to show the effect of handedness clearly. RH spirals give rise to polarization azimuth rotation angles  $\delta_0 \sim -11.6^\circ, -12.7^\circ,$  and  $-15.1^\circ$

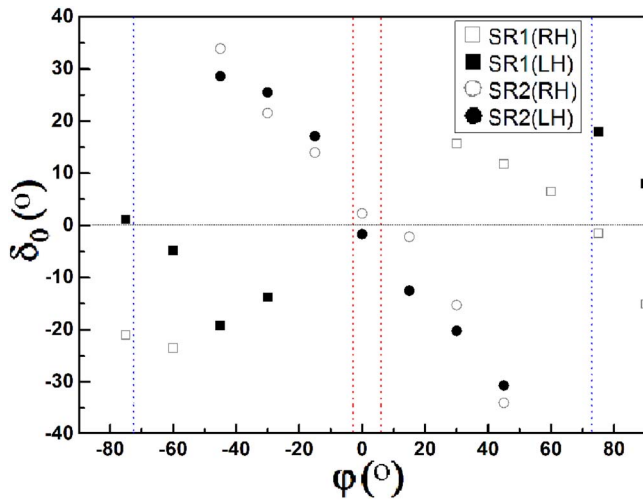


FIG. 4. (Color online) Measured polarization rotation  $\delta_0$  of SR1 and SR2 modes for RH and LH spirals with  $\Lambda=21 \mu\text{m}$  vs the initial polarization angle  $\varphi$ . The dashed line is the approximate position where  $\delta_0=0$ .

(counterclockwise), while LH spirals give rise to opposite sign of  $\delta_0=11.7^\circ$ ,  $11.8^\circ$ , and  $8.0^\circ$  (clockwise) for chiral period  $\Lambda=27$ ,  $24$ , and  $21 \mu\text{m}$ , respectively. Since the resolution of the transmission data is  $10^\circ$ , it is reasonable to conclude that the polarization rotation of SR1 is independent on the lattice period. In other words, the results in Fig. 3 should be the same even considering a single spiral slot. Note that a partial overlapping of the SP peak and SR1 (at  $94 \mu\text{m}$ ) in the transmission spectrum will occur only at array period  $\Lambda=27 \mu\text{m}$ . The calculated ellipticities are of an average magnitude  $|\eta|_{\text{avg}}=12.6^\circ$ . The results of light transmission from the front and back (RH and LH) are completely reversed. However, it will be shown later that this is only a special case for SR1 at  $\varphi=90^\circ$ . Nevertheless, this behavior is distinct to the optical activity that the sign of rotation should not depend on the direction of incident light.

Figure 4 shows the calculated polarization rotation  $\delta_0$  for SR1 and SR2 for  $\Lambda=21 \mu\text{m}$  as a function of the initial polarization orientation  $\varphi$  from  $-90^\circ$  to  $90^\circ$  for RH and LH spirals. It reveals that  $\delta_0$  changes smoothly as the initial polarization azimuth  $\varphi$  varies. More importantly, two specific polarization orientations  $\varphi$  defined as  $\varphi_{\text{node}}$  are found for SR1 and SR2, respectively, where no rotation are allowed ( $\delta_0=0^\circ$ ). The  $\varphi_{\text{node,RH}}$  and  $\varphi_{\text{node,LH}}$  for SR1 mode in RH and LH spirals are at  $\sim 75^\circ$  and  $-75^\circ$  (blue dotted line), respectively. The  $\varphi_{\text{node,RH}}$  and  $\varphi_{\text{node,LH}}$  for SR2 mode in RH and LH spirals are at  $\sim 5^\circ$  and  $-5^\circ$  (red dotted line), respectively. A more astonishing result as looking into Figs. 2(a) and 2(b), where  $\varphi \sim \varphi_{\text{node}}$  also corresponds to the highest transmission for peak SR1 and SR2. It is quite straightforward that  $\varphi_{\text{node}}$  has an opposite sign for opposite handedness since the pre-

ferred polarization orientation to excite the corresponding SR mode is also *flipped* which is confirmed by LH transmission results (not shown).

It is obvious that  $\varphi_{\text{node}}$  plays the most important role in determining the polarization rotation. If the initial linear polarization light is aligned with  $\varphi_{\text{node}}$  no polarization rotation is observed. Therefore, the polarization rotation for the SR of the spirals is a result of its polarization dependent transmission. This mechanism is similar to those apertures such as rectangular and elliptical holes that have strong polarization dependence although the spiral is much more complex. For example, the polarization dependence of transmission in Fig. 2 where  $\varphi_{\text{node,RH}}$  for SR1  $\sim 75^\circ$  can be effectively viewed as if the major axis of the ellipse is tilted  $75^\circ$  from its  $p$ -polarization  $[0,1]$ .<sup>1</sup> Moreover, the sign of rotation could be predicted as soon as  $\varphi_{\text{node}}$  is identified from the transmission spectrum.

In summary, the polarization rotation by a thin metal film perforated with Archimedean spiral slots is demonstrated. It is found that the polarization effects for transmission and rotation all depends on the initial polarization orientation. A special angle  $\varphi_{\text{node}}$  for SR mode is found that represents a preferred polarization orientation without polarization rotation. These observations could be used to design optical devices such as filters and polarizers or manipulate the polarization of light in a distinct and unusual way.

This work has been supported by the National Science Council of the Republic of China for financial support under Contract No. NSC 96-2221-E-002-242.

- <sup>1</sup>R. Gordon, A. G. Brolo, A. McKinnon, A. Rajora, B. Leathem, and K. L. Kavanagh, *Phys. Rev. Lett.* **92**, 037401 (2004).
- <sup>2</sup>M.-W. Tsai, T.-H. Chuang, H.-Y. Chang, and S.-C. Lee, *Appl. Phys. Lett.* **89**, 093102 (2006).
- <sup>3</sup>J. W. Lee, M. A. Seo, D. J. Park, D. S. Kim, S. C. Jeoung, Ch. Lienau, Q.-H. Park, and P. C. M. Planken, *Opt. Express* **14**, 1253 (2006).
- <sup>4</sup>E. Hecht, *Optics* (Addison-Wesley, Reading, MA, 2002).
- <sup>5</sup>V. A. Fedotov, P. L. Mladyonov, S. L. Prosvirnin, A. V. Rogacheva, Y. Chen, and N. I. Zheludev, *Phys. Rev. Lett.* **97**, 167401 (2006).
- <sup>6</sup>A. S. Schwanecke, V. A. Fedotov, V. V. Khardikov, S. L. Prosvirnin, Y. Chen, and N. I. Zheludev, *Nano Lett.* **8**, 2940 (2008).
- <sup>7</sup>T. Vallius, K. Jefimovs, J. Turunen, P. Vahimaa, and Y. Svirko, *Appl. Phys. Lett.* **83**, 234 (2003).
- <sup>8</sup>M. Kuwata-Gonokami, N. Saito, Y. Ino, M. Kauranen, K. Jefimovs, T. Vallius, J. Turunen, and Y. Svirko, *Phys. Rev. Lett.* **95**, 227401 (2005).
- <sup>9</sup>K. Konishi, T. Sugimoto, B. Bai, Y. Svirko, and M. Kuwata-Gonokami, *Opt. Express* **15**, 9575 (2007).
- <sup>10</sup>K. Konishi, B. Bai, X. Meng, P. Karvinen, J. Turunen, Y. P. Svirko, and M. Kuwata-Gonokami, *Opt. Express* **16**, 7189 (2008).
- <sup>11</sup>D. K. Wickenden, R. S. Awadallah, P. A. Vichot, B. M. Brawley, E. A. Richards, J. W. M. Spicer, M. J. Fitch, and T. J. Kistenmacher, *IEEE Trans. Antennas Propag.* **55**, 2591 (2007).
- <sup>12</sup>T. W. Ebbesen, H. J. Lezec, H. F. Ghaemi, T. Thio, and P. A. Wolf, *Nature (London)* **391**, 667 (1998).